ROBUST MULTICARRIER SPREAD SPECTRUM TECHNIQUE FOR DATA TRANSMISSION OVER PARTIALLY JAMMED CHANNELS

Behrouz Farhang-Boroujeny and Cynthia Furse
Department of Electrical and Computer Engineering, University of Utah

ABSTRACT

Multicarrier spread spectrum (MC-SS) is an alternative to the conventional spread spectrum (SS) techniques that behaves significantly better when the system is subject to narrow- or partial-band interference. However, successful implementation of the optimum detector requires knowledge of noise and interference variance in each subcarrier band. In this correspondence, we propose a suboptimal detector for MC-SS that keeps the significant gain of MC-SS over the conventional SS, with a relatively low loss compared to the optimum MC-SS detector. Theoretical analysis and computer simulations that corroborate the theory are presented.

I. INTRODUCTION

Jam-resistant communication is traditionally established through direct sequence spread spectrum (DS-SS) and frequency hopping spread spectrum (FH-SS) techniques. More recently, multi-carrier spread spectrum (MC-SS) techniques have also been identified, and their performance advantages over the conventional spread spectrum (SS) schemes have been explored [1], [2], [3]. It has been particularly noted that MC-SS is significantly more robust against narrow-band and partial-band interference/jamming. However, to achieve the predicted performance, the receiver should constantly monitor the powers of noise and interference at all the subcarriers. This might be a difficult task in a hostile environment where noise and interference may be non-stationary. In particular, an intelligent narrow-band jammer may hop in an unpredictable manner over different subcarriers.

This paper proposes a robust MC-SS technique with performance near that of the optimum detector without requiring any knowledge of the interference and noise powers. The proposed system can thus work in hostile environments where prediction of the powers of noise and interference might be difficult.

Different variations of the MC-SS system are possible. Kaleh [2] has considered a case where the spreading/processing gain, G, is equal to the number of subcarriers, N, and has proposed spreading a data symbol across all subcarriers as in Fig. 1. When (maybe, due to design limitations) $N < G$, a data symbol may be spread both across time and frequency [1]. Other variations are also possible [3], [4]. In this paper, we limit ourselves

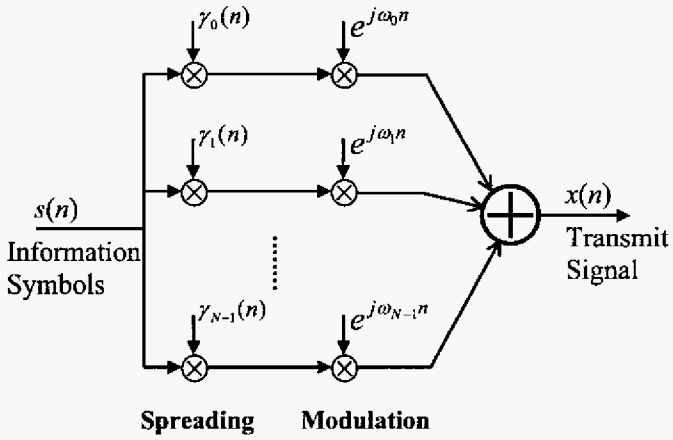

Fig. 1. Transmitter structure of a multicarrier spread spectrum system.

to the MC-SS scheme proposed and studied by Kaleh [2]. However, we note that our results are extendable to other variations of the MC-SS systems as well. We also note that different authors have used different names for reference to what is defined in this paper as MC-SS. Kaleh [2] has used the terminology '*frequency-diversity spread-spectrum*', while '*multicarrier DS CDMA*' is used in [1]. We use MC-SS as it relates better the common terminology DS-SS.

It has commonly been noted that to allow successful rejection of narrowband interference in a MC-SS system, the system subbands must be well isolated from each other [1], [2], [3], [5]. To achieve this, transmission is established through disjoint subbands. This is different from the conventional multicarrier modulation systems, such as orthogonal frequency division multiplexing (OFDM) [6], where there is significant overlap among different subbands. The analysis performed in [1], [2], [3] assumes perfect isolation of the subbands. In this paper, also, we make the same assumption.

This paper is organized as follows. In Section II, the channel model and the optimum detector are introduced. The suboptimum detector is proposed in Section III. An analysis of the proposed detector is also presented in this section. In Section IV, a scenario for comparing the proposed detector with the optimum MC-SS and DS-SS detectors is discussed. Computer simulations that confirm the accuracy of the theoretical analysis are also presented. The concluding remarks are presented

0-7803-8847-X/04/$20.00 ©2004 IEEE

in Section V.

Throughout the paper the following notations are adhered to. Scalar variables are denoted by lower-case non-bold letters. Lower-case bold letters are used to refer to column vectors. Matrices are denoted by upper-case bold letters. The ith element of a vector $\mathbf{x}$ is denoted by x_i. The superscripts T and H denotes transpose and Hermitian, respectively. $E[\cdot]$ denote statistical expectation.

II. Channel Model and the Optimum Detector

As was noted above, a variety of combinations of multicarrier and spread spectrum techniques is possible. In this paper we consider the case where a data symbol $s(n)$ has been spread across N subcarriers, as shown in Fig. 1, through a spreading vector $\boldsymbol{\gamma}(n) = [\gamma_0(n)\ \gamma_1(n)\ \cdots\ \gamma_{N-1}(n)]^T$ where $\gamma_i(n)$'s are a set of complex numbers that may be fixed or vary with time, n. Assuming that the channels associated with different subcarriers are flat-fading and non-overlapping, the received signal after demodulation and separation of the subcarrier components results in the vector [2]

$$\mathbf{r}(n) = s(n)\mathbf{H}\boldsymbol{\gamma}(n) + \boldsymbol{\nu}(n) \tag{1}$$

where $\mathbf{H}$ is a diagonal matrix with the channel gain of different subcarriers as its diagonal elements, and $\boldsymbol{\nu}(n)$ is the vector of channel noise plus interference/jammer.

Given the received vector $\mathbf{r}(n)$, we wish to obtain a soft estimate $\hat{s}_o(n)$ of the data symbol $s(n)$ through an optimum linear processing procedure. To this end, we rearrange (1) as

$$\mathbf{r}'(n) = s(n)\mathbf{u} + \boldsymbol{\nu}'(n) \tag{2}$$

where $\mathbf{u}$ is a vector of length N with elements of 1, $\mathbf{r}'(n) = (\mathbf{H}\boldsymbol{\Gamma}(n))^{-1}\mathbf{r}(n)$, $\boldsymbol{\nu}'(n) = (\mathbf{H}\boldsymbol{\Gamma}(n))^{-1}\boldsymbol{\nu}(n)$, and $\boldsymbol{\Gamma}(n)$ is the diagonal matrix whose diagonal elements are the elements of $\boldsymbol{\gamma}(n)$. Assuming that the noise plus interference vector $\boldsymbol{\nu}(n)$ is Gaussian[1] and, for $m \neq n$, $\boldsymbol{\nu}(m)$ and $\boldsymbol{\nu}(n)$ are independent of each other, the optimum linear estimation of $s(n)$, is given by

$$\hat{s}_o(n) = \mathbf{w}_o^H \mathbf{r}'(n) \tag{3}$$

where $\mathbf{w}_o$ is chosen such that the signal-to-interference plus noise ratio (SINR) is maximized.

The SINR is maximized through the following constrained minimization:

$$\mathbf{w}_o = \arg\min E[|\mathbf{w}^H\boldsymbol{\nu}'(n)|^2], \quad \text{subject to the constraint} \tag{4}$$

Here, the constraint $\mathbf{w}^H\mathbf{u} = 1$ assures that $E[\hat{s}_o(n)] = s(n)$, and the minimization of $E[|\mathbf{w}^H\boldsymbol{\nu}'(n)|^2]$ results in minimum variance in the estimation error. This problem can be solved by using the method of Lagrange multipliers [8], [9]. The result is

$$\mathbf{w}_o = \frac{1}{\mathbf{u}^T\mathbf{R}_{\nu'\nu'}^{-1}\mathbf{u}}\mathbf{R}_{\nu'\nu'}^{-1}\mathbf{u} \tag{5}$$

where $\mathbf{R}_{\nu'\nu'} = E[\boldsymbol{\nu}'(n)\boldsymbol{\nu}'^H(n)]$. Moreover, the variance of the estimation error is obtained as $E[|\mathbf{w}_o^H\boldsymbol{\nu}'(n)|^2] = 1/(\mathbf{u}^T\mathbf{R}_{\nu'\nu'}^{-1}\mathbf{u})$. Hence, assuming that $E[|s(n)|^2] = 1$, the SINR at the decision device input is obtained as

$$\rho_o = \frac{E[|s(n)|^2]}{E[|\mathbf{w}_o^H\boldsymbol{\nu}'(n)|^2]} = \mathbf{u}^T\mathbf{R}_{\nu'\nu'}^{-1}\mathbf{u}. \tag{6}$$

The optimum estimator (5) provides a solution to the optimum detector without any restriction on the correlation properties of noise and interference. The previous reports, such as [2], consider special cases of the above result. To compare the results here with those of [2], consider the case where the channel noise is flat across the full band of transmission and has the per subcarrier band power N_o. Also, assume that a subset of subchannels are jammed by an interferer with per subcarrier band power J_o. We also assume that $|\gamma_i(n)| = 1$, for all values of i, and $E[|s(n)|^2] = 1$. When the subcarrier bands are non-overlapping, $\mathbf{R}_{\nu\nu}$ is a diagonal matrix and, in the present case, has the diagonal elements of N_o for the un-jammed subchannels and $N_o + J_o$ for the jammed subchannels. In this case from (5), we obtain

$$w_{o,i} = \frac{\frac{|h_i|^2}{N_o+\alpha_i J_o}}{\sum_{k=0}^{N-1}\frac{|h_k|^2}{N_o+\alpha_k J_o}}, \quad i = 0, 1, \cdots, N-1 \tag{7}$$

where $w_{o,i}$ is the ith element of $\mathbf{w}_o$, and α_i is a binary number 0 or 1 showing absence or presence of the jammer, respectively, in the ith subchannel. Moreover, using (6), the SINR in this case is obtained as

$$\rho_o = \sum_{k=0}^{N-1}\frac{|h_k|^2}{N_o + \alpha_k J_o}. \tag{8}$$

When $|h_k| = 1$, for $k = 0, 1, \cdots, N-1$, the latter case reduces to the case considered in [2], and the conclusions derived in [2] will follow.

III. Suboptimum Detector

The above results show that the optimum detector requires knowledge of the spreading code, $\gamma_i(n)$, the channel gain, h_i, of each subchannel and also the noise and interference statistics. From these $\gamma_i(n)$ is obviously known to a detector that is designed to receive the transmitted SS signal. Estimation of the channel gains h_i's is also possible in most of the applications where the channel varies slowly with time. The most challenging

[1] An interference signal/jammer, in general, may be non-Gaussian. However, when it is a random process spread across a number of subcarrier bands, the demodulation (a multiband filtering process) results in a set of approximately Gaussian random variables.

problem that makes realization of the optimum detector very difficult is estimation of the noise and interference powers at each subchannel. In this section, we deviate from the optimum detector and propose a suboptimum detection method that performs close to the optimum detector, yet does not require any knowledge of the noise and interference power spectral densities.

Our method is based on a heuristic. We assume that the data symbols $s(n)$ have a constant modulo of one, i.e., when phase shift keying (PSK) signalling is used (the most common case in SS systems), and argue that the expected values of the magnitude of each element of $\mathbf{r}'(n)$ is unity. We thus normalize the elements of $\mathbf{r}'(n)$ to a length of unity prior to the linear processing. This normalization is implemented as

$$\tilde{r}_i(n) = \frac{r_i'(n)}{|r_i'(n)|}, \quad i = 0, 1, \cdots, N-1. \tag{9}$$

A. Analysis of $\tilde{r}_i(n)$

In SS systems it is very common to choose $s(n)$ from a PSK alphabet. Moreover, the suboptimum detector that we propose in this section performs well only when $s(n)$ is PSK. We thus limit our discussion to the cases where $|s(n)| = 1$. Moreover, to facilitate some of the derivations below, with no loss of generality, we assume that $s(n) = 1$. Extension to the cases where $s(n) \neq 1$ is straightforward and will be discussed later.

We start the analysis by studying $r_i'(n)$. For this, we define the random variables $x_i = 1 + \Re\{\nu_i'(n)\}$ and $y_i = \Im\{\nu_i'(n)\}$, where $\Re\{\cdot\}$ and $\Im\{\cdot\}$, respectively, denote the real part and the imaginary part of the argument. Note that since here we assume $s(n) = 1$, x_i and y_i are real and imaginary parts of $r_i'(n)$, respectively. Noting that $\nu_i'(n)$ is a complex zero-mean circularly symmetric Gaussian random variable, the joint probability density function (PDF) of x_i and y_i is obtained as

$$f_{x_i y_i}(x_i, y_i) = \frac{1}{2\pi\sigma_i'^2} e^{-((x_i-1)^2+y_i^2)/2\sigma_i'^2} \tag{10}$$

where $\sigma_i'^2$ is the variance of $\nu_i'(n)$. Next, we define the random variables $z_i = \sqrt{x_i^2 + y_i^2}$ and $\varphi_i = \arctan(y_i/x_i)$. The joint PDF of z_i and φ_i is given by (see [7], page 145)

$$f_{z_i\varphi_i}(z_i, \varphi_i) = \frac{z_i}{2\pi\sigma_i'^2} e^{-(z_i^2+1-2z_i\cos\varphi_i)/2\sigma_i'^2}. \tag{11}$$

The marginal PDF of φ_i is thus

$$f_{\varphi}(\varphi_i) = \int_0^\infty f_{z\varphi_i}(z, \varphi_i) dz. \tag{12}$$

Substituting (11) in (12), after some manipulations, we obtain

$$f_{\varphi_i}(\varphi_i) = \frac{1}{2\pi} e^{-\frac{1}{2\sigma_i'^2}} + \frac{\cos\varphi_i e^{-\frac{\sin^2\varphi_i}{2\sigma_i'^2}}}{2\sqrt{2\pi}\sigma_i'} \left(1 + \text{sign}(\cos\varphi_i)\text{erf}\left(\frac{|\cos\varphi_i|}{\sqrt{2}\sigma_i'}\right)\right) \tag{13}$$

where $\text{sign}(\cdot)$ is the signum function and $\text{erf}(\cdot)$ is the error function $\text{erf}(x) = \frac{2}{\sqrt{\pi}} \int_0^x e^{-t^2} dt$.

On the other hand, we note that when $s(n) = 1$, the real and imaginary parts of $\tilde{r}_i(n)$ are $\cos\varphi_i$ and $\sin\varphi_i$, respectively. Defining the random variables $p_i = \cos\varphi_i$ and $q_i = \sin\varphi_i$ and following standard methods for functions of random variables [7], the PDF's of p_i and q_i, over the interval $[-1, 1]$, are obtained as

$$f_{p_i}(p_i) = \frac{e^{-1/2\sigma_i'^2}}{\pi\sqrt{1-p_i^2}} + \frac{p_i e^{-(1-p_i^2)/2\sigma_i'^2}}{\sqrt{2\pi}\sigma_i'\sqrt{1-p_i^2}} \left(1 + \text{sign}(p_i)\text{erf}\left(\frac{|p_i|}{\sqrt{2}\sigma_i'}\right)\right) \tag{14}$$

and

$$f_{q_i}(q_i) = \frac{e^{-1/2\sigma_i'^2}}{\pi\sqrt{1-q_i^2}} + \frac{e^{-q_i^2/2\sigma_i'^2}}{\sqrt{2\pi}\sigma_i'} \text{erf}\left(\frac{\sqrt{1-q_i^2}}{\sqrt{2}\sigma_i'}\right). \tag{15}$$

The above results are summarized as follows. When $s(n) = 1$, the normalized observation sample $\tilde{r}_i(n)$ is a random variable whose real and imaginary parts are characterized by the random variables p_i and q_i with PDF's given by (14) and (15), respectively. When $s(n) \neq 1$, but still has a modulo of one, i.e., $|s(n)| = 1$, by writing $\tilde{r}_i(n) = s(n)\frac{1+\nu_i'(n)/s(n)}{|1+\nu_i'(n)/s(n)|}$ and noting that the random variables $\nu_i'(n)$ and $\nu_i'(n)/s(n)$ have the same statistics, we conclude that $\tilde{r}_i(n)/s(n)$ is a random variable whose real and imaginary parts are also characterized by the random variables p_i and q_i. One important corollary of this result is that

$$E[\tilde{r}_i(n)] = s(n)E[p_i]. \tag{16}$$

B. Optimal Detector for $\tilde{\mathbf{r}}(n)$

The optimal detector for the normalized observation vector $\tilde{\mathbf{r}}(n) = [\tilde{r}_0(n)\ \tilde{r}_1(n)\ \cdots\ \tilde{r}_{N-1}(n)]^T$ is obtained as follows. We first scale each element $\tilde{r}_i(n)$ such that its mean is equal to $s(n)$. Using (16), we find that the scaling factor that establishes this is $1/E[p_i]$. Let us call the scaled version of $\tilde{\mathbf{r}}(n)$, $\check{\mathbf{r}}(n)$ and the associated noise vector $\check{\boldsymbol{\nu}}(n)$. Considering $\check{\mathbf{r}}(n)$ to be the observation vector, the optimum detector is obtained by following the same line of derivation that led to (5). This leads to the estimate

$$\check{s}(n) = \check{\mathbf{w}}_o^H \check{\mathbf{r}}(n) \tag{17}$$

where $\breve{\mathbf{w}}_o = \frac{1}{\mathbf{u}^T \mathbf{R}_{\breve{\nu}\breve{\nu}}^{-1} \mathbf{u}} \mathbf{R}_{\breve{\nu}\breve{\nu}}^{-1} \mathbf{u}$ and $\mathbf{R}_{\breve{\nu}\breve{\nu}} = E[\breve{\boldsymbol{\nu}}(n)\breve{\boldsymbol{\nu}}^H(n)]$.

We note that since $\breve{\nu}(n)$ is non-Gaussian, the latter detector is not an optimum linear estimator of $s(n)$, in the strict sense of minimizing the detection error. However, it is optimum in the minimum mean-square error (MMSE) sense, i.e., it minimizes $E[|\breve{s}(n) - s(n)|^2]$. Moreover, since the estimation error $\breve{s}(n) - s(n) = \breve{\mathbf{w}}_o^H \breve{\boldsymbol{\nu}}(n)$ is a linear combination of a set of random variables, it approaches a Gaussian distribution for large values of the processing gain N, and thus the MMSE estimator will approach the true optimum detector, i.e., the one that minimizes the probability of symbol errors.

C. A Practical Suboptimum Detector

The detector defined by (17), even though optimal for the observed vector $\breve{\mathbf{r}}(n)$, defeats our goal of proposing a suboptimum detector that does not require any knowledge of the noise and interference powers. Construction of $\breve{\mathbf{r}}(n)$ and thus $\breve{\mathbf{w}}_o$ requires knowledge of the noise and interference powers in each subchannel, since the statistics of p_i and q_i depend on $\sigma_i'^2$ which in turn is a function of the noise and interference powers.

Since no knowledge of the distribution of noise and interference is available, it is reasonable to assume that all subchannels are corrupted by the same amount of noise plus interference. That is, the elements of $\boldsymbol{\nu}(n)$ have the same variance, σ^2. Assuming that the subcarrier bands are non-overlapping [1], [2], we get $E[\boldsymbol{\nu}(n)\boldsymbol{\nu}^H(n)] = \sigma^2\mathbf{I}$. Using this, we find that $\mathbf{R}_{\nu'\nu'}$ is a diagonal matrix with the ith diagonal element of $\sigma_i^2 = \frac{\sigma^2}{|h_i|^2|\gamma_i(n)|^2}$.

Next, we use the PDF's (14) and (15) to find an estimate of the diagonal elements of $\mathbf{R}_{\breve{\nu}\breve{\nu}}$ for substitution in (17). To this end, we first note that the assumption "non-overlapping subcarrier bands" implies that $\mathbf{R}_{\breve{\nu}\breve{\nu}}$ is a diagonal matrix. Let $\sigma_{p_i}^2$ and $\sigma_{q_i}^2$ denote the variances of random variables p_i and q_i, respectively. Recalling the construction of $\breve{\mathbf{r}}(n)$, one finds that the ith diagonal element of $\mathbf{R}_{\breve{\nu}\breve{\nu}}$ is given by

$$\breve{\sigma}_i^2 = \frac{\sigma_{p_i}^2 + \sigma_{q_i}^2}{(E[p_i])^2} = \frac{1 - (E[p_i])^2}{(E[p_i])^2} \tag{18}$$

where the second identity follows from $\sigma_{p_i}^2 + \sigma_{q_i}^2 = E[p_i^2] - (E[p_i])^2 + E[q_i^2] - (E[q_i])^2 = E[p_i^2 + q_i^2] - (E[p_i])^2 = 1 - (E[p_i])^2$, since $E[q_i] = 0$ because of even symmetry of the PDF of q_i (see (15)), and $p_i^2 + q_i^2 = \sin^2\phi_i + \cos^2\phi_i = 1$.

Unfortunately, because of the presence of the error function in (14), derivation of an analytical equation for $E[p_i]$ and thus (18) is not possible. However, it can be evaluated numerically. Fig. 2 shows $\breve{\sigma}_i^2$ as a function of $\frac{\sigma^2}{|h_i|^2}$. Surprisingly, this very closely resembles a linear relationship,[2] implying the identity

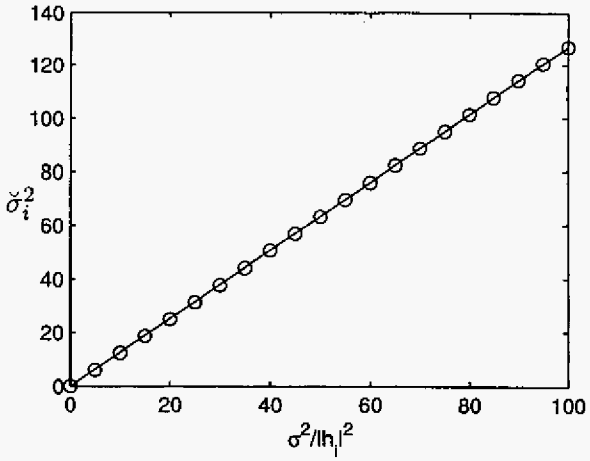

Fig. 2. Relationship between $\sigma^2/|h_i|^2$ and $\breve{\sigma}_i^2$. The circles show the points that have been evaluated numerically. The line is the best linear fit. The slope of the line is $K = 1.269$.

$$\breve{\sigma}_i^2 = \frac{K\sigma^2}{|h_i|^2}. \tag{19}$$

where $K = 1.269$ is the slope of the line in Fig. 2. Substituting (19) in (17), we obtain

$$\breve{\mathbf{w}}_{\text{subo}} = \frac{1}{\sum_{i=0}^{N-1} |h_i|^2} \begin{bmatrix} |h_0|^2 \\ |h_1|^2 \\ \vdots \\ |h_{N-1}|^2 \end{bmatrix} \tag{20}$$

where the subscript 'subo' denotes sub-optimum. Hence, the suboptimum estimate $\breve{s}_{\text{subo}} = \breve{\mathbf{w}}_{\text{subo}}^H \breve{\mathbf{r}}(n)$ is obtained. However, this requires $\breve{\mathbf{r}}(n)$ that in turn requires values of $E[p_i]$ which are dependent on σ^2. Since σ^2 (summation of noise and interference powers) is unknown, one cannot claim the possibility of constructing $\breve{\mathbf{r}}(n)$.

To resolve the above problem, we resort to a detector that uses $\tilde{\mathbf{r}}(n)$ instead of $\breve{\mathbf{r}}(n)$. To this end, we note that substituting (19) in (18) gives

$$E[p_i] = \frac{|h_i|}{\sqrt{K\sigma^2 + |h_i|^2}}. \tag{21}$$

Since the cases of interest in SS systems are when SINR is very small and in such cases $|h_i|^2 \ll K\sigma^2$, from (21), we obtain $E[p_i] \approx \frac{|h_i|}{\sigma\sqrt{K}}$. Using this and recalling the definition of $\breve{\mathbf{r}}(n)$, one finds that

$$\breve{s}_{\text{subo}}(n) \approx \frac{\sigma\sqrt{K}}{\sum_{i=0}^{N-1} |h_i|^2} \sum_{i=0}^{N-1} |h_i| \tilde{r}_i(n). \tag{22}$$

[2]Although, not clear in Fig. 2, the linear relationship between $\frac{\sigma^2}{|h_i|^2}$ and $\breve{\sigma}_i^2$ is lost at lower values of $\frac{\sigma^2}{|h_i|^2}$, corresponding to higher values of SINR. However, since in practical applications of SS, cases of interest are low SINR's (usually negative SINR's) only, the use of linear relationship (19) is justified.

Moreover, since we assume PSK signaling and such signaling is insensitive to a positive scaling, the factor on front of the summation on the right-hand side of (22) may be removed. This leads to the desired suboptimum estimate

$$\tilde{s}_{\text{subo}}(n) = \sum_{i=0}^{N-1} |h_i| \tilde{r}_i(n). \tag{23}$$

D. Summary of the Suboptimum Detector

Table I presents a summary of the proposed detector. As one may notice, this a very simple detector that requires only the spreading factors $\gamma_i(n)$ and the channel gains h_i. It is interesting to note that the scaled samples $\breve{r}_i(n)$ do not appear in the detector. They only played an intermediate role in obtaining the final estimate (23).

TABLE I

SUMMARY OF THE SUBOPTIMUM DETECTION ALGORITHM.

1. Alignment:	$r'_i(n) = \dfrac{r_i(n)}{h_i \gamma_i(n)}$ for $i = 0, 1, \cdots, N-1$
2. Normalization:	$\tilde{r}_i(n) = \dfrac{r'_i(n)}{\lvert r'_i(n) \rvert}$ for $i = 0, 1, \cdots, N-1$
3. Symbol Estimation:	$\tilde{s}_{\text{subo}}(n) = \sum_{i=0}^{N-1} \lvert h_i \rvert \tilde{r}_i(n)$

E. SINR Analysis

We note that $\tilde{r}_i(n) = E[p_i]\breve{r}_i(n) = E[p_i](s(n) + \breve{\nu}_i(n))$. Substituting this in (23), we obtain $\tilde{s}_{\text{subo}}(n) = \theta s(n) + \nu_{\text{subo}}(n)$, where $\theta = \sum_{i=0}^{N-1} |h_i| E[p_i]$ and $\nu_{\text{subo}}(n) = \sum_{i=0}^{N-1} |h_i| E[p_i] \breve{\nu}_i(n)$. Since $|s(n)| = 1$, the SINR of the suboptimum detector is thus obtained as

$$\begin{aligned} \rho_{\text{subo}} &= \frac{\theta^2}{E[|\nu_{\text{subo}}(n)|^2]} \\ &= \frac{\left(\sum_{i=0}^{N-1} |h_i| E[p_i]\right)^2}{\sum_{i=0}^{N-1} |h_i|^2 (E[p_i])^2 \breve{\sigma}_i^2} \\ &= \frac{\left(\sum_{i=0}^{N-1} |h_i| E[p_i]\right)^2}{\sum_{i=0}^{N-1} |h_i|^2 \left(1 - (E[p_i])^2\right)} \end{aligned} \tag{24}$$

where the last identity follows from (18).

To allow comparison of the proposed suboptimum detector with the optimum detector proposed in Section II, we follow the noise-jammer setup that was discussed at the end of Section II and simplify ρ_{subo} accordingly. We note that for the noise-jammer setup of Section II, (21) converts to

$$E[p_i] = \frac{|h_i|}{\sqrt{K(N_o + \alpha_i J_o) + |h_i|^2}}. \tag{25}$$

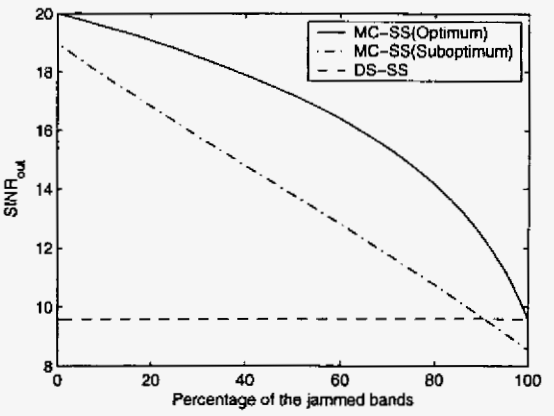

(a)

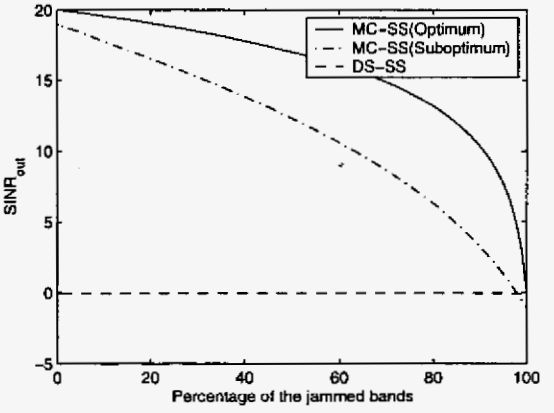

(b)

Fig. 3. SINR performance comparison of the optimum MC-SS, the suboptimum MC-SS, and DS-SS. SNR = 0 dB. (a) The total power of jammer is 10 dB above the noise level. (b) The total power of jammer is 20 dB above the noise level.

Substituting (25) in (24), we get

$$\rho_{\text{subo}} = \frac{\left(\sum_{i=0}^{N-1} \frac{|h_i|^2}{\sqrt{K(N_o+\alpha_i J_o)+|h_i|^2}}\right)^2}{\sum_{i=0}^{N-1} \frac{|h_i|^2 K(N_o+\alpha_i J_o)}{K(N_o+\alpha_i J_o)+|h_i|^2}}. \tag{26}$$

IV. COMPARISONS

In this section, we present some numerical results that compare the performance of the suboptimum detector (23) with the optimum detector (3). Also, for comparison, we present the performance of a DS-SS system with the same processing gain. We note that DS-SS performs similar to the optimal MC-SS when all subchannels/chips are subject to the same level of noise plus interference. However, as was noted in Section I, DS-SS performs significantly worse than MC-SS when both are subject to partial-band interference [1], [2].

Results in this section are for a flat fading channel, i.e., h_i's are all equal. We assume that subcarrier bands are

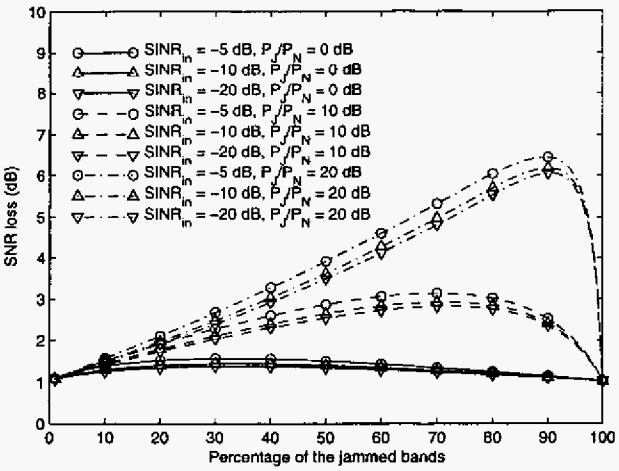

Fig. 4. SNR loss of the suboptimum detector compared to the optimum detector.

perfectly isolated from one another. Results are presented for the processing gain $N = 100$. Also, with no loss of generality, we set $|h_i| = 1$, for $i = 0, 1, \cdots, N-1$. Moreover, we set $|s(n)| = |\gamma_i(n)| = 1$, for all values of n and i. We assume that M of the subcarrier bands are corrupted by the interference. We also define the signal-to-interference, signal-to-noise and signal-to-interference plus noise ratios

$$\begin{aligned} \mathrm{SIR_{in}} &= \frac{\sum_{i=0}^{N-1} E[|h_i\gamma_i(n)s(n)|^2]}{M \times J_o} \\ &= \frac{N}{MJ_o} \end{aligned} \tag{27}$$

$$\begin{aligned} \mathrm{SNR_{in}} &= \frac{\sum_{i=0}^{N-1} E[|h_i\gamma_i(n)s(n)|^2]}{N \times N_o} \\ &= \frac{1}{N_o} \end{aligned} \tag{28}$$

$$\begin{aligned} \mathrm{SINR_{in}} &= \frac{\sum_{i=0}^{N-1} E[|h_i\gamma_i(n)s(n)|^2]}{N \times N_o + M \times J_o} \\ &= \frac{1}{N_o + (M/N)J_o} \end{aligned} \tag{29}$$

where the subscript 'in' is to emphasize that the ratios are given for the signals at the receiver input. Both channel noise and interference are modeled by Gaussian sources.

For our study in this section, it is convenient to refer to the values of N, M, $\mathrm{SIR_{in}}$, $\mathrm{SNR_{in}}$ and $\mathrm{SINR_{in}}$, as a starting point. When N and M and two of the ratios $\mathrm{SIR_{in}}$, $\mathrm{SNR_{in}}$ or $\mathrm{SINR_{in}}$ are given, we can use (27)-(29) to calculate the noise variance N_o and the interference variance J_o. These can then be substituted in (8) and (26) to obtain ρ_o and ρ_{subo}.

Figs. 3(a) and (b) show two sets of plots of SINR's ρ_o, (8), and ρ_{subo}, (26), as a function of the percentage of the SS band that is corrupted by interference. In both cases $\mathrm{SNR_{in}} = 0$ dB. In Fig. 3(a), $\mathrm{SIR_{in}} = -10$ dB, while in Fig. 3(b), $\mathrm{SIR_{in}} = -20$ dB. As expected, when

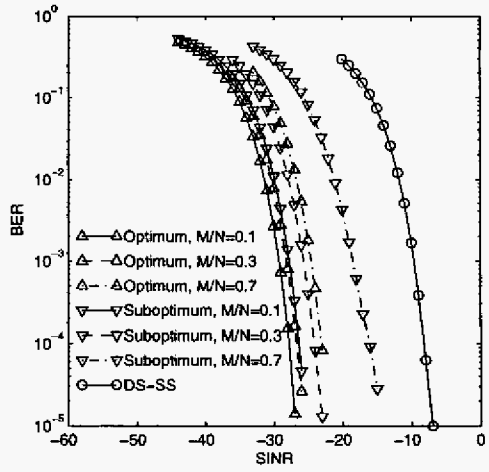

(a)

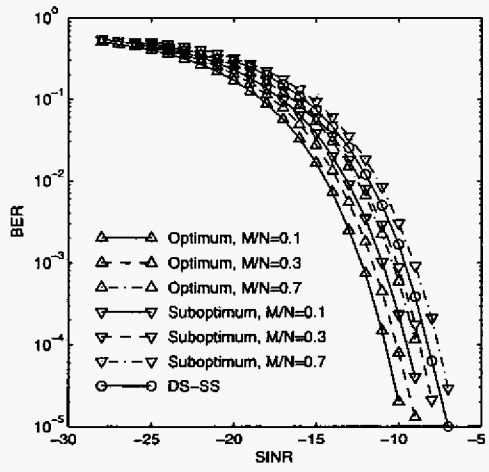

(b)

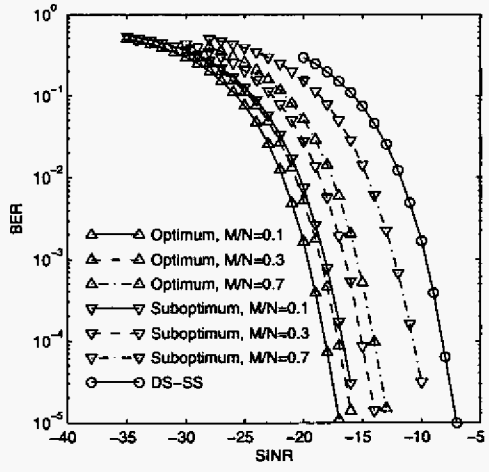

(c)

Fig. 5. Bit error rates of the optimum and suboptimum MC-SS as a function of SINR, when (a) $P_J/P_N = 20$ dB, (b) $P_J/P_N = 10$ dB and (c) $P_J/P_N = 0$ dB. The BER of DS-SS is also presented for comparison.

a small fraction of the SS band is jammed, MC-SS performs significantly better than DS-SS. This advantage vanishes as the jammer energy is spread over a larger portion of the band. The suboptimum detector loses about 1 dB compared to the optimum detector, when the jammer occupies either a small fraction or 100% of the transmission band. Larger losses are observed when a larger fraction of the band, but not the full-band, is jammed. Nevertheless, the suboptimum MC-SS performs significantly better than DS-SS, unless the band is fully jammed.

Fig. 4 presents performance loss, $\rho_o/\rho_{\text{subo}}$, incurred due to replacement of the optimum detector by the suboptimum detector. Results for several combinations of SINR_{in} and the ratio of interference power to noise power P_J/P_N, where $P_J = MJ_o$ and $P_N = NN_o$ are the total interference power and the total noise power, respectively, are given. The parameter that has the most impact on the shapes of the curves is the ratio P_J/P_N. The curves depend on SINR_{in} to a much smaller extent.

To corroborate the accuracy of the predictions made by (8) and (26), in Figs. 5(a), (b) and (c) we have presented a set of bit-error-rate (BER) curves of the optimum and suboptimum detectors for P_J/P_N values of 20 dB, 10 dB and 0 dB, respectively. Quadrature phase-shit keying (QPSK) symbols are considered and gray coding has been applied to map data bits to symbols. Each point on the curves is calculated after observing at least 500 bit errors. The performance loss of the suboptimum detector compared to the optimum detector in these figures matches very closely the prediction made in Fig. 4. For instance, according to Fig 4 a difference of 1 to 6 dB should be observed between the optimum and suboptimum detectors when $P_J/P_N = 20$ dB, and this difference should increase as M/N varies between 0 and 0.9. This is clearly observed in Fig. 5(a). Moreover, with decreasing P_J/P_N, the difference between the optimum and suboptimum detector reduces. This trend is observed in Figs. 5(b) and (c).

V. Conclusion

An effective, but simple, method of implementing MC-SS systems in a hostile environment, where an intelligent jammer may hop to different subcarriers randomly, was proposed and its performance was analyzed theoretically. The proposed scheme, does not require knowledge of this jammer and even though suboptimum, was found to be significantly superior to the conventional DS-SS. Computer simulations that confirm the accuracy of the theoretical results were also presented. Even though the presented results do not cover many possible conditions where the channel may be frequency selective and/or noise and interference spectrums may have arbitrary shapes, the conclusions drown remain the same. Namely, when the received signal is corrupted by a partial band interference, the proposed detector performs significantly better than the DS-SS system. Moreover, the system degradation compared to the optimum MC-SS detector is usually in the range of 1 to a few decibels.

References

[1] S. Kondo, and L. B. Milstein, "Performance of multicarrier DS CDMA systems," *IEEE Trans. Communications.*, vol. 44, no. 2, Feb. 1996, pp. 238-246.

[2] G. K. Kaleh, "Frequency-diversity spread-spectrum communication system to counter bandlimited Gaussian interference,"*IEEE Trans. Communications,* vol. 44, no. 7, July 1996, pp. 886-893.

[3] K. Cheun, K. Choi, H. Lim, and K. Lee, "Antijamming performance of a multicarrier direct-sequence spread-spectrum system," *IEEE Trans. Communications,* vol. 47, no. 12, Dec. 1999, pp. 1781-1784.

[4] S. Hara and R. Prasad, "Overview of multicarrier CDMA," *IEEE Communications Magazine*, vol. 35, no. 12, Dec. 1997, pp. 126-133.

[5] E. Lemois and F. Buda, "New advances in multi-carrier spread spectrum techniques for tactical communications," In Proceedings of *IEEE Military Communications Conference*, 1998, MILCOM 98, vol. 2,18-21 Oct. 1998, pp. 664 -668.

[6] R. Van Nee, and R. Prasad, *OFDM for Wireless Multimedia Communications.* Boston, MA: Arthec House, 2000.

[7] A. Papoulis, *Probability, Random Variables, and Stochastic Processes.*, McGraw-Hill, 2nd ed., 1984.

[8] T. K. Moon and W. C. Stirling, *Mathematical Methods and Algorithms for Signal Processing.* Prentice-Hall, Upper Saddle River, NJ, 2000.

[9] B. Farhang-Boroujeny, *Adaptive Filters: Theory and Applications.* John Wiley and Sons, 1998.